Security Classification

DOCUMENT CONTROL DATA - R & D

(Security classification of title, body of abstract and indexing annotation must be entered when the overall report is classified)

1. ORIGINATING ACTIVITY (Corporate author)	2a. REPORT SECURITY CLASSIFICATION
Naval Research Laboratory Washington, D.C. 20390	Unclassified
	2b. GROUP

3. REPORT TITLE

FRACTURE TOUGHNESS OF FILAMENT-WOUND COMPOSITES
PART I—EFFECT OF MATERIAL VARIABLES

4. DESCRIPTIVE NOTES (Type of report and inclusive dates)

A final report on one phase of the problem.

5. AUTHOR(S) (First name, middle initial, last name)

Robert J. Sanford
Fred R. Stonesifer

6. REPORT DATE	7a. TOTAL NO. OF PAGES	7b. NO. OF REFS
July 29, 1970	22	8

8a. CONTRACT OR GRANT NO.	9a. ORIGINATOR'S REPORT NUMBER(S)
NRL Problems F01-14 and F01-04	NRL Report 7112
b. PROJECT NO. Projects 544-102-12432 and	
c. RR 009-03-45-5451	9b. OTHER REPORT NO(S) (Any other numbers that may be assigned this report)
d.	

10. DISTRIBUTION STATEMENT

This document has been approved for public release and sale; its distribution is unlimited

11. SUPPLEMENTARY NOTES	12. SPONSORING MILITARY ACTIVITY
	Department of the Navy (Office of Naval Research and Naval Ship Systems Command), Arlington, Va. 22217

13. ABSTRACT

The application of the theory of linear fracture mechanics to quasi-brittle, glass-reinforced-plastic composites is an important first step in understanding the basic mechanisms of failure of these materials. In this study, a simple test technique sensitive to small changes in the material and/or environmental variables is developed based on fracture mechanics concepts.

Using the stress-intensity factor K_{Ic} as the evaluating parameter, six different resin-glass combinations were tested. The results of these tests indicate that (a) there is no difference in the fracture strength of composites made with either E-glass or S-glass, (b) composites with 5-mil-diam fibers have a lower resistance to crack propagation than those with conventional 0.4-mil-diam fibers, and (c) a filament-wound composite has a much lower fracture toughness in the B-staged state than in the fully cured state.

In another phase of this study, the effect of water immersion was investigated. These tests demonstrate that with the exception of the composite made with the large-diameter (5-mil) fibers there is no systematic decline in fracture strength due to water immersion for periods up to 6 months.

DD FORM 1 NOV 65 1473 (PAGE 1)

S/N 0101-807-6801

Security Classification

14. KEY WORDS	LINK A		LINK B		LINK C	
	ROLE	WT	ROLE	WT	ROLE	WT
Composites Fracture mechanics Fracture toughness						

CONTENTS

ABSTRACT

The application of the theory of linear fracture mechanics to quasi-brittle, glass-reinforced-plastic composites is an important first step in understanding the basic mechanisms of failure of these materials. In this study a simple test technique, sensitive to small changes in the material and/or environmental variables, is developed based on fracture mechanical concepts.

Using the stress-intensity factor K_{Ic} as the evaluating parameter, six different resin-glass combinations were tested. The results of these tests indicate that (a) there is no difference in the fracture strength of composites made with either E-glass or S-glass, (b) composites with 5-mil-diam fibers have a lower resistance to crack propagation than those with conventional 0.4-mil-diam fibers, and (c) a filament-wound composite has a much lower fracture toughness in the B-staged state than in the fully cured state.

In another phase of this study the effect of water immersion was investigated. These tests demonstrate that with the exception of the composite made with the large-diameter (5-mil) fibers there is no systematic decline in fracture strength due to water immersion for periods up to 6 months.

PROBLEM STATUS

This is a final report on one phase of the problem; work on other phases is continuing.

AUTHORIZATION

NRL Problems F01-14 and F01-04
Projects 544-102-12432 and RR 009-03-45-5451

Manuscript submitted April 6, 1970.

FRACTURE TOUGHNESS OF FILAMENT-WOUND COMPOSITES

PART I—EFFECT OF MATERIAL VARIABLES

INTRODUCTION

The use of glass-reinforced plastic (GRP) as the primary structural material for internally loaded pressure vessels has become an accepted practice for many aerospace applications because of its favorable strength-to-weight ratio. The possibility of using GRP for externally loaded pressure vessels for hydrospace applications is currently under consideration.

Present conventional test methods often measure structural properties which are dependent on the type of specimen and do not measure a basic parameter that is either applicable to all test methods or could be used in structural design. Since crack propagation is the primary mechanism of failure in the quasi-brittle GRP materials, the development of a test method for the measurement of resistance to crack propagation is a logical choice for investigating the effect of numerous variables on the strength of the resultant GRP. In addition, such a test method will provide an initial step in developing a technique for applying fracture-mechanics principles in the design of composite structures.

The studies reported here were undertaken to develop a relatively simple test method based on the principles of linear fracture mechanics which could be used to investigate the influence of changes in the materials and environmental variables on the strength of a composite material. The influence of changes in the component variables, including type of glass, size of filaments, resin system, and extent of cure, were investigated to determine the utility of the test method developed. Also, the influence of several external variables (moisture and direction of load application) was evaluated.

SPECIMEN DESIGN

All of the composites used in this program, with the exception of the one with large-diameter fibers, were fabricated on the NRL filament-winding machine. To ensure uniformity of composition and curing conditions for each resin-glass combination, it was desirable to fabricate all of the material of a given type for the entire series of tests in a single winding. This was accomplished by winding a cylinder 18 in. in diameter, 24 in. long and 0.1 in. in thickness of each different combination, resulting in approximately 1000 sq in. of each material from which specimens could be fabricated. The cylinder was then cut into 1.5-in.-wide hoops. The specimens were prepared from small sectors of each hoop. In addition to conserving material, the use of small specimens also tended to minimize the effect of curvature.

The existing fracture-toughness test methods developed for flat, isotropic plates and beams could not conveniently be applied to GRP materials; thus, a new fracture-toughness test suitable for the type of material under consideration had to be developed. As yet, no general theory exists for the analysis of the crack-propagation behavior of filament-wound composite materials with an arbitrary winding angle; however, the failure of unidirectional composites can be analyzed with the existing theory of fracture mechanics,

since crack extension is achieved by the formation of plane surfaces and can be completely described by the single parameter, crack length. Also, the unidirectional composite is probably a more sensitive indicator of the influence of changes in materials and environmental variables than any other layup angle, since the reinforcing effect of the fibers is minimized. Consequently, unidirectional composites were used exclusively throughout the program, all of the specimens being loaded so as to produce failure parallel to the glass filaments. Because of the curvature of the specimens in the direction of the filaments, the application of the load through small-diameter pins simplified the design of loading fixtures and allowed free rotation of the specimen during the test. Edge-notched specimens were chosen over center- or surface-notched ones because of the relative ease of fabrication.

The double-edge-notched specimen is well known and widely used for determining fracture-toughness values in isotropic materials. However, this configuration requires more material and more care in fabrication than some other types of specimens. Symmetry about the axis of loading must be strictly maintained both to eliminate bending moments and to ensure crack growth in a single plane. Maintaining symmetry is particularly critical in these small specimens.

The single-edge-notched specimen is less expensive to fabricate, requires less material, and contains only one crack front. In this type of specimen the stress at the root of the notch results from a combination of applied tension and bending moment; thus, the symmetry requirements are much less severe.

Several techniques were evaluated for the fabrication of the tip of the notch. Ultrasonic matching was not satisfactory, as the heat generated charred the material locally. A jeweler's saw tended to pull the fibers from the faces of the specimen, leaving small surface flaws and cracks at the root of the notch. A water-cooled abrasive cutoff wheel did not damage the specimen, but could not produce a small enough radius at the tip of the notch. An acceptable notch was formed by first using the cutoff wheel to make most of the notch and then completing the notch with a sharply pointed diamond wheel. With such a notch, the crack always originated at the tip of the small radius portion of the notch and gave consistent results.

For the specimen configurations shown in Fig. 1, the opening mode stress-intensity factor K_{Ic} can be expressed as (1)

$$K_{Ic} = \frac{P}{t\sqrt{\pi \ell}} \tag{1a}$$

for the double-edge-notched specimen, and

$$K_{Ic} = \frac{P}{t\sqrt{\pi \ell}} \left(0.67295 + 2.71287 \frac{e}{\ell} \right) \tag{1b}$$

for the single-edge-notched specimen,

where

P = load at failure

t = thickness of specimen

2ℓ = length of net section

e = eccentricity of the loading relative to the center of the net section.

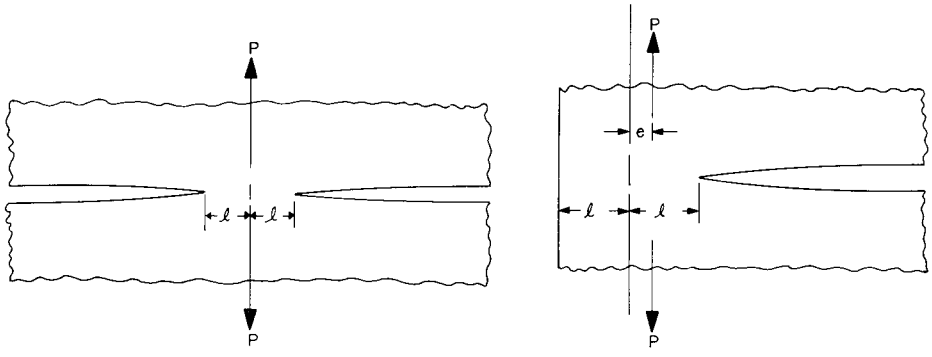

(a) infinite plate with symmetric edge notches

(b) half-plate with a notch approaching the free edge

Fig. 1 - Specimen configurations used as the basis for the mathematical analysis

An alternate measure of the fracture toughness is the strain energy release rate $\mathcal{G}_c$, which can be computed for any specimen configuration by the compliance method (2,3). For either specimen configuration, the strain-energy rate is obtained from

$$\mathcal{G}_c = -\frac{p^2}{4}\frac{d(\delta/p)}{d\ell}, \tag{2}$$

where

δ/p = compliance of the specimen per unit thickness

p = load at failure per unit thickness.

However, the quantities K_{Ic} and $\mathcal{G}_c$ are not independent measures of the fracture toughness. Irwin (4) has shown that

$$\mathcal{G}_c = CK_{IC}^2, \tag{3}$$

where C is a function of the elastic constants of the material.

As stated earlier, the height of the specimen was chosen as 1-1/2 in. in order to conserve material. The maximum length of the net section was limited by the strength of the specimens through the loading-pin holes. Preliminary tests indicated that a net section length of 0.5 in. or less in double-edge-notched specimens produced no failures at the loading pins. A length of 0.75 in. or less in a single-edge-notched specimen with an eccentricity of 0.125 in. produced similar results.

The remaining dimension, the width of the specimen, had to be chosen so as to approximate the requirement of infinite width used in the derivation of Eqs. (1). To determine the minimum specimen width which would satisfy this criteria, a series of tests was conducted with single-edge-notched specimens having an eccentricity of 0.125 in., net section length of 0.75 in., and widths of 1, 1-1/2, and 2 in. The results of these tests, using Eq. (1b), showed a marked increase in K_{Ic} in going from 1 to 1-1/2 in. in width, but negligible change between 1-1/2 and 2 in. in width.

A similar series of tests on double-edge-notched specimens showed constant values of K_{Ic} for specimens 3 in. wide and larger.

Based on these tests, 1-1/2-in.-wide, single-edge-notched specimens and 3-in.-wide, double-edge-notched specimens, shown in Fig. 2, were considered acceptable and used throughout the testing program.

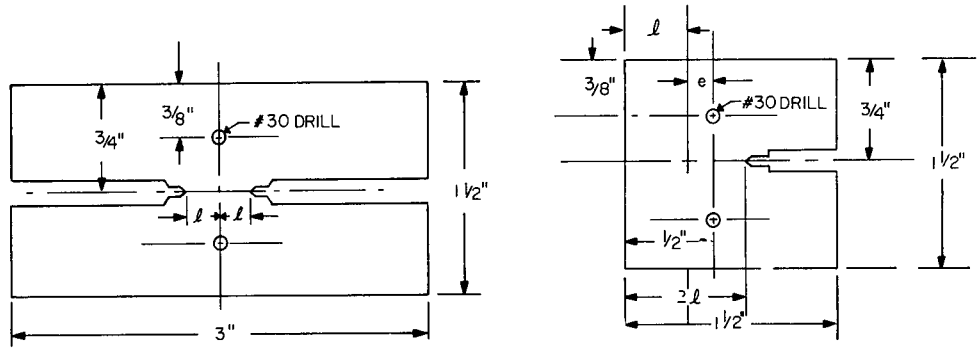

(a) double-edge-notched specimen (b) single-edge-notched specimen

Fig. 2 - Standardized test specimens

EFFECT OF MATERIAL VARIABLES

In this phase of the study, a series of tests was conducted to determine the effect of material variables on the fracture toughness of GRP materials under standardized test conditions. In all, six different resin-glass compositions were tested. From these six compositions, the change in K_{Ic} and δ_c resulting from changes in type of resin, type of hardener, type of glass, glass fiber diameter, and degree of cure were evaluated. Four of the six compositions are commercially available systems which either have been or could be used for structural purposes. One was fabricated with an experimental hardener, meta-aminobenzyl amine (MABA), by the Chemistry Division, NRL (5), and is not yet commercially available. The remaining composite consists of commercially available. The remaining composite consists of commercially available constituents, but the resin was given only a partial cure (B-staged). This composite, while not practical for structural applications, was included in the program to determine the effect of the extent of cure on the fracture toughness of the composite, particularly since burst tests on GRP bottles have shown only a minor degradation in ultimate burst strength with B-staged resin (6).

A summary of the composites used in this program is shown in Table 1, along with the measured resin contents and elastic moduli. The resin content was obtained by a burnout technique (Federal Specification L-P-406b, Method 7061). The elastic modulus was measured in tension in the direction transverse to the fibers.

Compliance tests for both types of specimens were conducted on each of the materials in Table 1, and the data were fitted by the least-squares method to a third-order polynomial from which $[d(\delta/p)]/d\ell$ was computed. Typical compliance curves for two separate tests are shown in Figs. 3 through 6. The symbols ⊙ and △ distinguish data from each test.

Table 1
Glass-Reinforced Plastics Evaluated

No.	Resin System		Glass		Resin by Weight (%)	Transverse Elastic Modulus ($\times 10^6$ psi)
	Source	Type	Diameter ($\times 10^{-3}$ in.)	Type		
1	Shell	Epon 826/CL	0.4	S-HTS	27.3	3.24
2	Union Carbide	ERL 2256/0820	0.4	E-HTS	23.0	3.10
3	Shell	Epon 826/CL	0.4	E-HTS	23.8	3.22
4	Union Carbide	ERL 2256/0820	5.0	E-HTS	16.4	5.22
5	Shell	Epon 826/CL (B - Stage only)	0.4	S-HTS	26.5	2.88
6	Shell	Epon 826/MABA*	0.4	S-HTS	27.4	3.26

*MABA prepared by Chemistry Division, NRL.

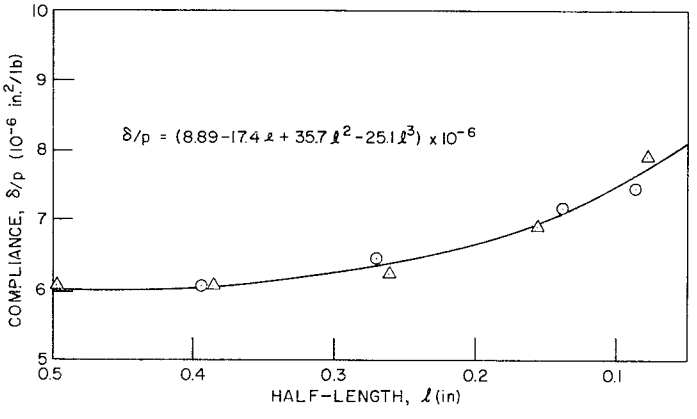

Fig. 3 - Typical compliance vs net section length curve for a double-edge-notched specimen made with fine fibers (Epon 826/CL, E-HTS glass, 0.4-mil diameter)

The results of the fracture-toughness tests are shown in Table 2 and also in Fig. 7. Each value is the average of 24 tests. All tests were performed in a controlled environment of 75°F and 45% RH at a loading rate of 0.020 in./min.

On completion of this series of tests, a "t" test for significance of the difference between the means was conducted. The results of this analysis indicate that the difference in the average fracture toughness resulting from each change of a material's variable are significant at the 99+% level in all cases except for the change in the type of glass.

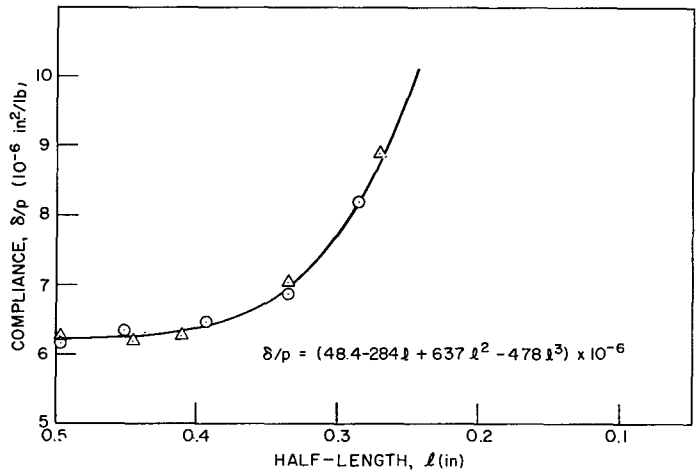

Fig. 4 - Typical compliance vs net section length curve for a single-edge-notched specimen made with fine fibers (Epon 826/CL, E-HTS glass, 0.4-mil diameter)

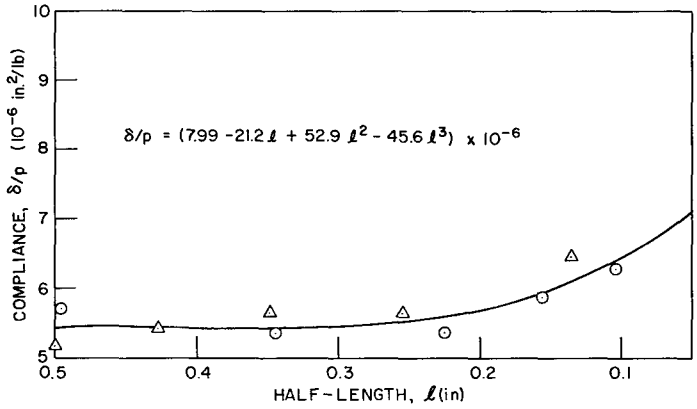

Fig. 5 - Typical compliance vs net section length curve for a double-edge-notched specimen made with coarse fibers (ERL 2256/0820, E-glass, 5.0-mil diameter)

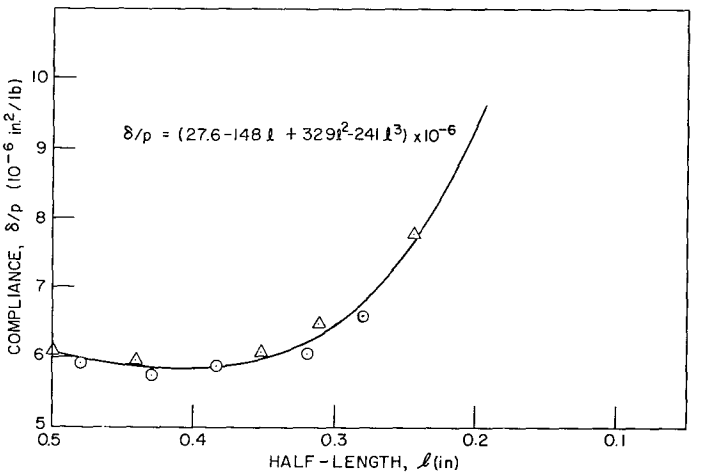

Fig. 6 - Typical compliance vs net section length curve for a single-edge-notched specimen made with coarse fibers (ERL 2256/0820, E-glass, 5.0-mil diameter)

Table 2
Fracture Toughness Properties of Glass-Reinforced Plastics

No.	Resin System		Glass		Single-Edge-Notched Specimen		Double-Edge-Notched Specimen	
	Source	Type	Diameter ($\times 10^{-3}$ in.)	Type	K_{Ic} (psi $\sqrt{\text{in.}}$)	$\mathcal{G}_c$ (lb./in.)	K_{Ic} (psi $\sqrt{\text{in.}}$)	$\mathcal{G}_c$ (lb./in.)
1	Shell	Epon 826/CL	0.4	S-HTS	1270	0.9	1080	1.0
2	Union Carbide	ERL 2256/0820	0.4	E-HTS	1520	1.2	1310	1.3
3	Shell	Epon 826/CL	0.4	E-HTS	1340	1.6	1100	1.1
4	Union Carbide	ERL 2256/0820	5.0	E-HTS	1030	0.3	850	0.3
5	Shell	Epon 826/CL (B - Stage only)	0.4	S-HTS	320	0.5	270	0.3
6	Shell	Epon 826/MABA*	0.4	S-HTS	1480	2.8	1250	3.1

*MABA prepared by Chemistry Division, NRL.

Note: Each K_{Ic} and $\mathcal{G}_c$ value is the average from 24 specimens.

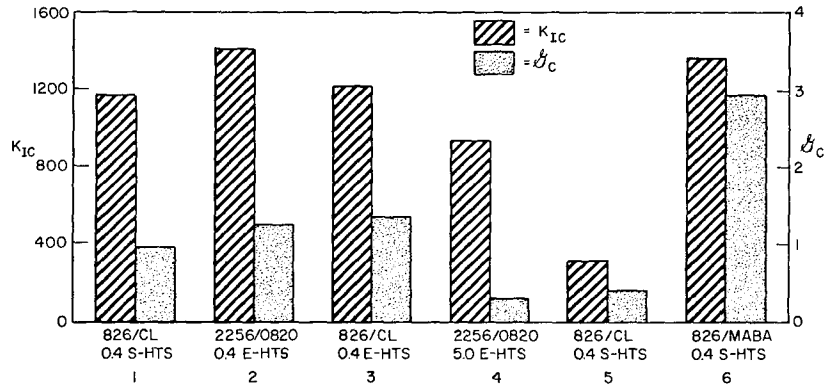

Fig. 7 - Results of the fracture toughness tests using the standardized specimens and tested in controlled environment (see also Table 2)

It should also be noted that in the case of the large-diameter fibers (5-mil diameter) the surface finish was not applied to the glass directly as in the other cases, but was instead mixed with the resin and applied during the winding operation. Since this was the only material which contained both the large-diameter fibers and the different method of applying the surface finish, the difference in the fracture toughness of this material must be attributed to the combined effect of these two variables and not to the change in a single variable as in all of the other cases. In addition, no attempt was made to rigidly control the resin content other than to use a uniform procedure for winding all of the specimens.

Within these limitations the following conclusions can be drawn from the data:

(a) The test method is sensitive to changes in materials' variables and can be used to evaluate GRP materials on the basis of fracture toughness,

(b) No significant improvement in fracture toughness was observed when E-HTS glass was replaced with the higher strength S-HTS glass,

(c) MABA hardener produces a higher toughness composite than CL hardener when used with Epon 826 resin,

(d) A filament-wound composite has a much lower fracture toughness in the B-staged state than in the fully cured state,

(e) Fine-fiber (0.4-mil) composites have a higher fracture toughness than coarse-fiber (5.0-mil) composities, and

(f) The ERL 2256/0820 resin system produces a tougher composite than the Epon 826/CL resin system.

Several representative specimens were mounted, polished, and examined under a microscope. Typical micrographs for the fine- and coarse-fiber materials are shown in Figs. 8 and 9, respectively. These figures clearly show that the crack propagates by failure at or very near the resin-glass interface. Thus, the adhesion of the surface finish to both the resin and the glass plays a predominate role in the fracturing process of unidirectional glass-reinforced plastics.

Fig. 8 - Photomicrograph of a typical fracture in composites with 0.4-mil-diam fibers, demonstrating that the crack propagates by failure at or near the glass-resin interface

Fig. 9 - Photomicrograph of a typical fracture in composites with 5-mil-diam fibers, demonstrating that the crack propagates by failure at or near the glass-resin interface

EFFECT OF COMBINED NORMAL AND SHEAR FORCES

In addition to the opening mode of crack extension reported in the previous section, there are two other independent modes which are possible. These modes, depicted in Fig. 10, correspond to in-plane shear forces and antiplane shear forces and are called the forward shear mode and the parallel shear mode; respectively. Each of these modes possesses a characteristic critical stress-intensity factor K and strain-energy release rate $\mathcal{G}$. However, the measurement of these parameters is considerably more difficult in the shear modes than in the opening mode, and, for the most part, has been ignored. Unfortunately, in GRP structures the forward shear mode is a common mode of failure. For example, a polished cross section of a typical failure of a GRP cylinder under external pressure is shown in Fig. 11.

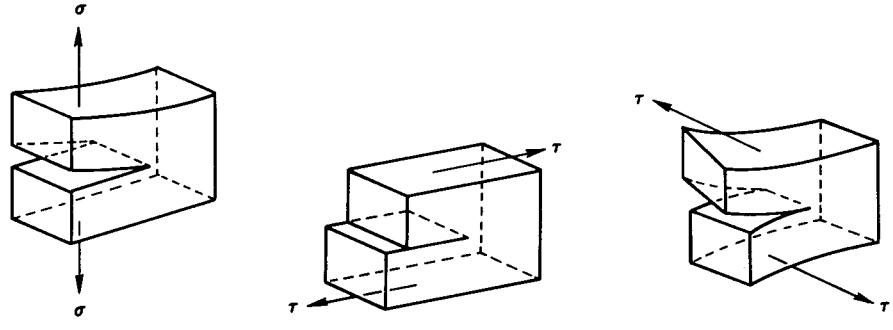

(a) K_I, opening mode

(b) K_{II}, forward shear mode

(c) K_{III}, parallel shear mode

Fig. 10 - The independent modes of crack propagation

If one postulates that the strain-energy release rate $\mathcal{G}$ is a bulk property of the material and thus is independent of the mode of loading, then the fracture toughness properties in the shear modes could be deduced from the opening mode results. The studies reported in this section were undertaken to determine the validity of this assumption.

If $\mathcal{G}$ is independent of the mode of loading, then the total strain-energy release rate is the sum of the release rates for each of the independent modes. Thus, for combined tension and forward shear

$$\mathcal{G} = \mathcal{G}_I + \mathcal{G}_{II} = \text{constant} . \tag{4}$$

By using equations analogous to Eq. (3),

$$\mathcal{G}_I = C_1 K_I^2 \tag{5a}$$

and

$$\mathcal{G}_{II} = C_2 K_{II}^2 , \tag{5b}$$

where C_1 and C_2 are both functions of the elastic compliances for the material. Therefore,

$$C_1 K_I^2 + C_2 K_{II}^2 = \text{constant} . \tag{6}$$

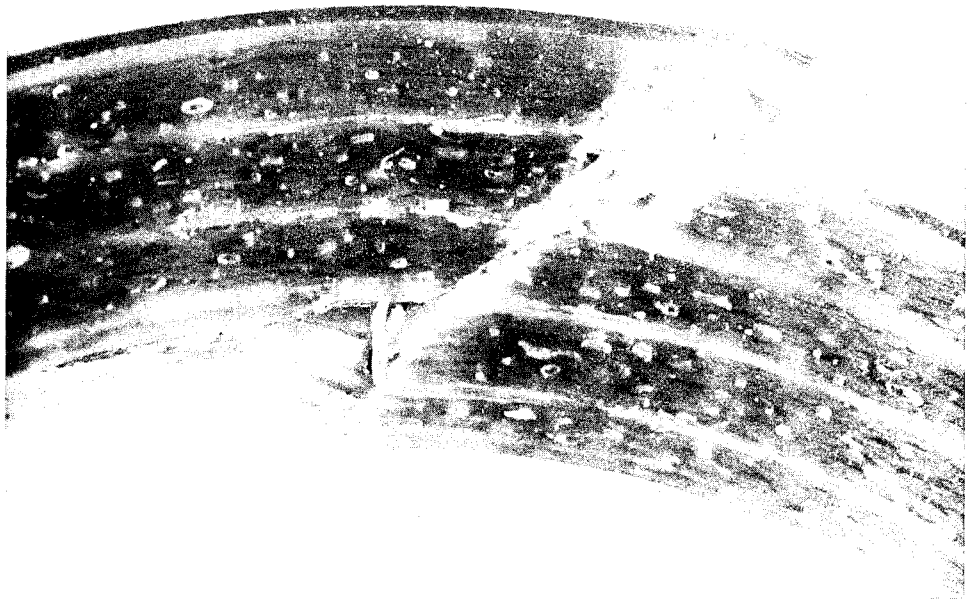

Fig. 11 - An example of the forward shear mode of failure in a GRP cylinder under external hydrostatic pressure

This equation is in the form of an ellipse with an axes ratio of $\sqrt[2]{C_1/C_2}$. For generalized plane stress it can be shown that (4)

$$\sqrt[2]{\frac{C_1}{C_2}} = \sqrt[4]{\frac{E_{11}}{E_{22}}}\ , \tag{7}$$

where E_{11} and E_{22} are the elastic moduli in the principal orthotropic directions.

The modified double-edge-notched specimen shown in Fig. 12 was utilized for the experimental verification of the postulate. Five different combinations of tension and shear loading were obtained by varying the angle of loading θ. The results of this investigation are shown in Fig. 13 (for a small-diameter fiber) and in Fig. 14 (for the large-diameter fiber); each data point represents the average of five specimens tested at that angle. The solid curve is the best-fit ellipse with axes as defined by the postulate. The ratio of elastic moduli was calculated from the percent by volume of glass content using Greszczuk's equations (7). Since all of the data are within 10% of the theoretical curve, there is sufficient evidence to accept the postulate that δ is an invariant with respect to the mode of loading. This means that fracture tests in the forward shear mode need not be performed, since the result can be deduced from the opening mode tests and the elastic properties. More importantly, the shear tests provide no new information about the fracture behavior of the material.

The above result is applicable when the normal component of load is tensile. For the case in which the normal component is compressive, Wu (8) demonstrated that the critical forward shear stress-intensity factor can be expressed as the sum of the stress-intensity factors due to the applied shear stress K_{II} and the resisting frictional shear stress K_{IIf}, which is proportional to the applied compressive stress. Therefore,

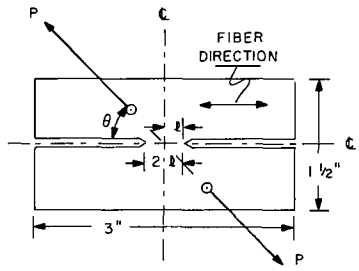

Fig. 12 - Modified double-edge-notched specimen used to study the effect of combined opening and forward shear modes of failure on the resultant strain energy release rate

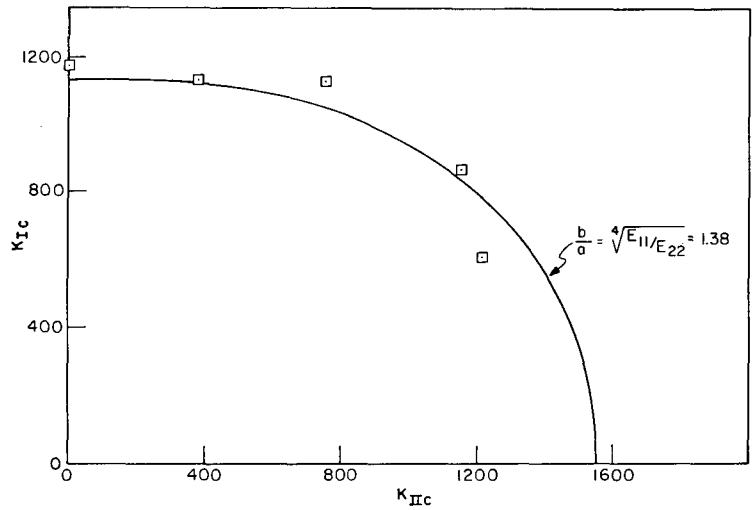

Fig. 13 - Verification of the postulate that $\mathcal{J}$ is an invariant with respect to the mode of loading for a fine fiber composite (Epon 826/CL, E-HTS glass, 0.4-mil diameter)

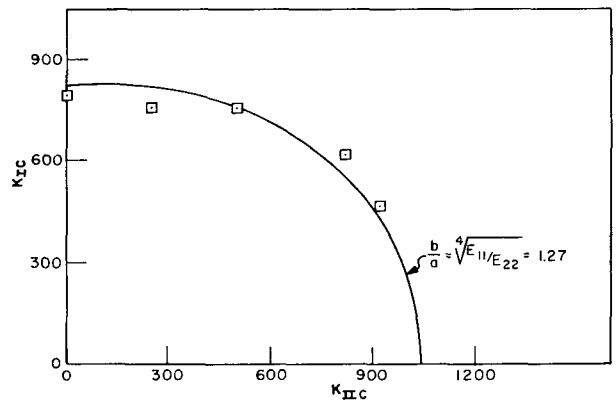

Fig. 14 - Verification of the postulate that $\mathcal{J}$ is an invariant with respect to the mode of loading for a coarse fiber composite (ERL 2256/0820, E-glass, 5.0-mil diameter)

$$K_{IIc} = K_{II} + K_{IIf} \quad (8)$$

Thus, due to the inhibiting action of the frictional forces, the critical stress-intensity factor in shear is larger when compressive loads are present, increasing linearly with the applied compressive stress.

EFFECT OF WATER IMMERSION

In this phase of the study, the effect of an extended period of water immersion on the critical opening mode stress-intensity factor K_{Ic} for each of the six materials was evaluated using single-edge-notched specimens as shown in Fig. 2. Specimens of each material were immersed in tap water at room temperature and allowed to soak for 8 days, 35 days, and 6 months, after which they were tested under each of four different test conditions.

The first group was tested immediately on removal from the water. The next group was air dried for 24 hours at room temperature and 40 to 70% RH before testing. The third group was removed from the water, an excess of water was injected into the notch, and the specimens were then tested. The final group of specimens was dried for 24 hours at 150°F, conditioned by 24 hours at room temperature and 40 to 70% RH, then tested.

In addition to these specimens, two control groups were also tested. One group from the same lot as the specimens which were water soaked was tested at room temperature and 40 to 50% RH, while the other control group, also from the same lot, was dried for 24 hours at 150°F, conditioned 24 hours at room temperature and 40 to 50% RH, and then tested. Each group of specimens mentioned above consisted of five specimens of each material. All tests were conducted at a loading rate of 0.05 in/min.

The results of these tests are given in Table 3 and also in graphical form in Figs. 15 through 20. There are several features of the data which deserve special mention. First, the B-staged material (Fig. 19) shows an apparent increase in strength with extended water immersion; but, this increase is probably due to the continued curing of the material. Second, the coarse-fiber material (Fig. 18) shows a drastic decline in strength. This degradation may be due to the method of applying the surface finish and should not be attributed to fiber diameter alone.

The remainder of the data, which include all of the fine-fiber materials with fully cured resin systems used in the program, shows no systematic decrease in fracture toughness resulting from water immersion for periods up to 6 months. These results indicate that degradation of crack propagation resistance caused by water immersion is not a general trait of GRP composites, but, instead, depends on the particular system under consideration.

SUMMARY

The purpose of this program was to develop suitable techniques for the application of fracture mechanics concepts to filament-wound GRP composites and to determine the effects of material and environmental variables on the resultant fracture toughness of these materials.

Initial efforts were directed toward developing the theory and experimental techniques for applying fracture mechanics concepts to filament-wound reinforced plastics. Test specimens were obtained from filament-wound rings, 18 in. in diameter and 1.5 in.

Table 3
Effect of Water Immersion on the Fracture Toughness of System Glass — Reinforced Plastics

Test Conditions	Time in Water (days)	#1 826/CL 0.4 S-HTS (psi $\sqrt{in.}$)	#2 2256/0820 0.4 E-HTS (psi $\sqrt{in.}$)	#3 826/CL 0.4 E-HTS (psi $\sqrt{in.}$)	#4 2256/0820 5.0 E-HTS (psi $\sqrt{in.}$)	#5 826/CL B-Staged 0.4 S-HTS (psi $\sqrt{in.}$)	#6 826/MABA 0.4 S-HTS (psi $\sqrt{in.}$)
Control, room temperature	0	1220	1480	1290	970	290	1420
Control, 150°F	0	1150	1420	1230	840	510	1220
Tested wet	8	1420	1640	1290	430	350	1390
	35	1130	1520	1200	60	430	1460
	180	1250	1390	1170	20	460	1360
Dried 24 hr at room temperature	8	1210	1450	1100	450	280	1390
	35	1100	1320	1060	90	550	1260
	180	1180	1410	830	60	590	1180
Tested with water in crack	8	1410	1730	1490	560	340	1670
	35	1360	1400	1220	70	530	1490
	180	1250	1610	1080	30	430	1280
Dried 24 hr at 150°F, 24 hr at room temperature	8	1220	1300	1050	400	740	1350
	35	1180	1260	1130	230	670	1480
	180	1280	1520	1180	100	520	1550

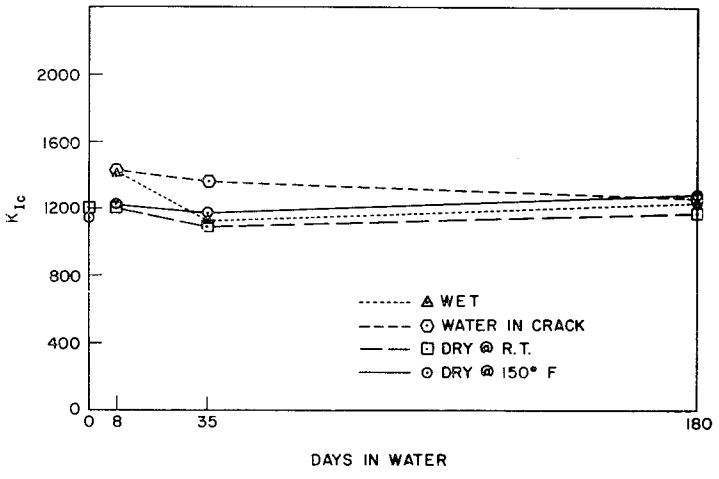

Fig. 15 - Effect of water immersion on the stress-intensity factor K_{Ic} for material 1 (see also Table 3) (Epon 826/CL, S-glass, 0.4-mil diameter)

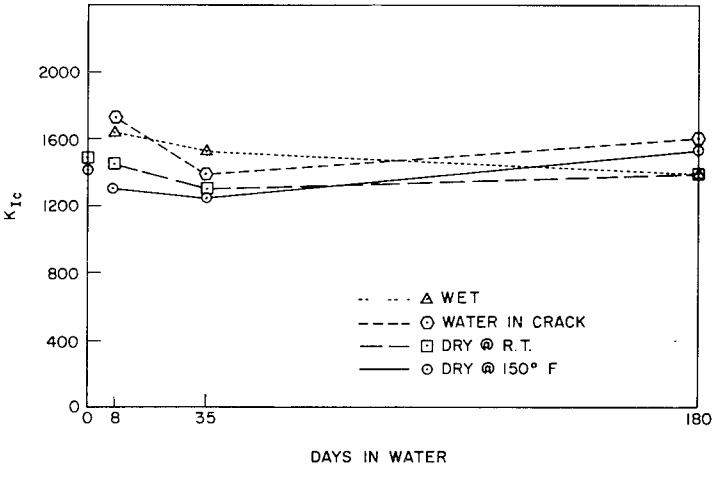

Fig. 16 - Effect of water immersion on the stress-intensity factor K_{Ic} for material 2 (see also Table 3) (ERL 2256/0820, E-glass, 0.4-mil diameter)

wide, which were cut into segments. Preliminary experiments led to the selection of two specimen configurations, a single-edge-notched and a double-edge-notched specimen (Fig. 2). A tensile load was applied to the specimen until the crack propagated. The stress-intensity factor K_{Ic} was calculated from the initial crack length, the maximum load, and the specimen geometry. The strain-energy release rate $\mathcal{G}_c$ was also calculated from specimen compliance measurements. The higher the value of either of these two parameters, the greater is the resistance to crack propagation.

In the first series of tests, component variables, including type of glass, size of filaments, resin system, and degree of cure were evaluated to determine the validity of the test method developed. The results are shown in Table 2. They indicate that the test method is reproducible and capable of differentiating between subsequent variables. They

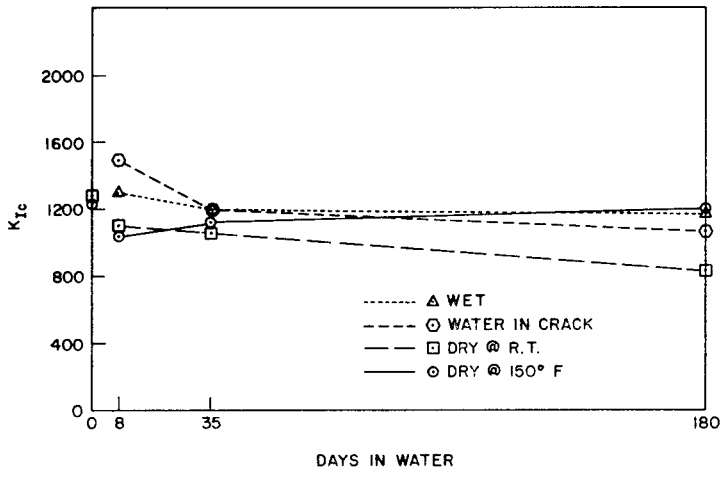

Fig. 17 - Effect of water immersion on the stress-intensity factor K_{Ic} for material 3 (see also Table 3) (Epon 826/CL, E-glass, 0.4-mil diameter)

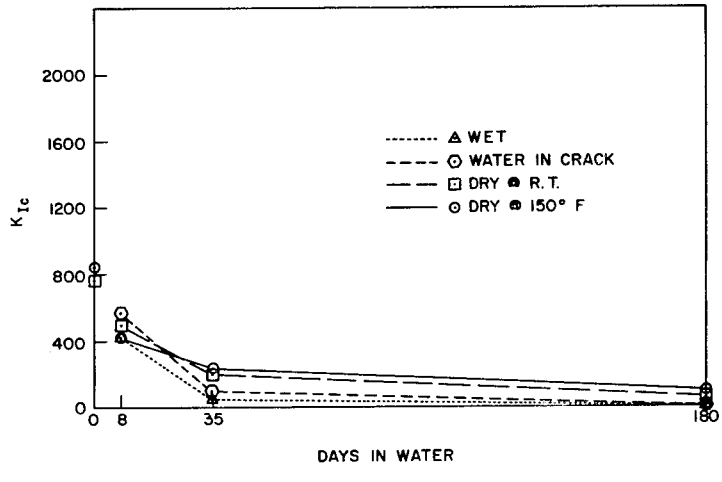

Fig. 18 - Effect of water immersion on the stress-intensity factor K_{Ic} for material 4 (see also Table 3) (ERL 2256/0820, E-glass, 5.0-mil diameter)

also show that (a) there is no difference in fracture toughness or crack propagation resistance of specimens made with E-glass as compared to those made with S-glass; (b) specimens made with 5-mil-diam fibers have a lower resistance to crack propagation than those made with conventional 0.4-mil-diam fibers. This may be due, at least in part, to the fact that the finish was applied to the 5-mil fibers in solution with the resin, rather than directly on the fibers. (c) Specimens made with a B-staged (undercured) resin have much lower resistance to crack propagation than those made with a fully cured resin. (d) The MABA hardener prepared in the Chemistry Division at NRL increases the toughness of the epoxy resin slightly.

A second series of tests was conducted to determine the effect of soaking in water up to 6 months on the crack propagation behavior of the same materials listed in Table 1.

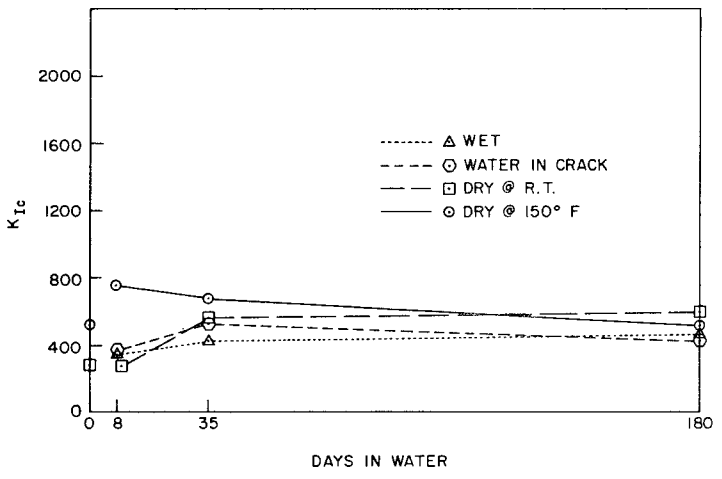

Fig. 19 - Effect of water immersion on the stress-intensity factor K_{I_c} for material 5 (see also Table 3) (Epon 826/CL, S-glass, 0.4-mil diameter, B-staged)

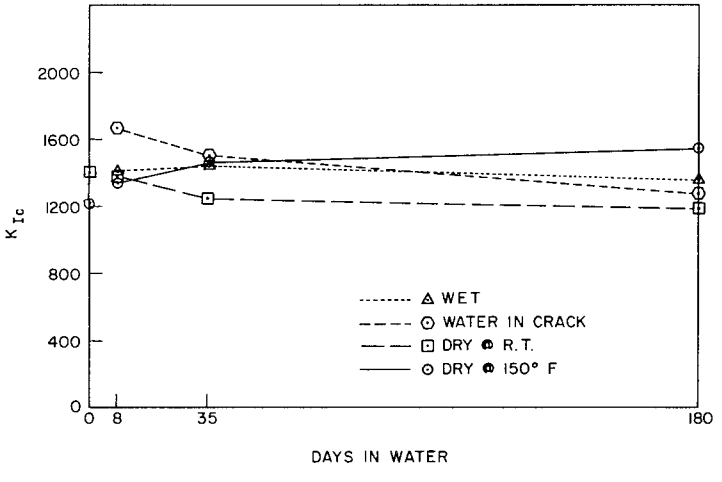

Fig. 20 - Effect of water immersion on the stress-intensity factor K_{I_c} for material 6 (see also Table 3) Epon 826/MABA, S-glass, 0.4-mil diameter)

The single-edge-notched specimen was used in these tests. There was considerable variability in the test results. Nevertheless, the tests indicated that the 6-months' water exposure did not decrease the crack propagation resistance of the epoxy-glass composites appreciably except in the case of the 5-mil filament composites. Again, the relatively poor behavior of these composites may well be associated with the manner of applying the glass finish — i.e., in the resin solution rather than directly to the glass surface.

In evaluating the failure behavior of composites using fracture mechanics concepts, it is possible to cause crack propagation by a pure tensile or opening mode type of loading or by two shear modes. It has been postulated that the strain-energy release rate $\mathcal{G}$ is independent of the mode of loading. If this assumption is valid, it is unnecessary to

evaluate the fracture toughness in the shear modes, since the values could be obtained from the simpler opening mode results. Studies were undertaken to determine the validity of this assumption. A modified double-edge-notch specimen was used in the experimental verification of this postulate. Five different combinations of tension and shear loading were obtained by varying the angle of loading. The results, shown in Figs. 13 and 14, indicate that δ is invariant with respect to the mode of loading, so that it is not necessary to separate strain-energy release rate into individual components.

REFERENCES

1. Paris, P.C., and Sih, G.C., "Stress Analysis of Cracks, "Fracture Toughness Testing and Its Applications," ASTM STP 381, American Society for Testing and Materials, Phila., Pa., p. 30, 1965

2. Irwin, G.R., "Fracture Testing of High-Strength Sheet Materials Under Conditions Appropriate for Stress Analysis," NRL Report 5486, July 27, 1960

3. Sullivan, A.M., "New Specimen Design for Plane-Strain Fracture Toughness Tests," Materials Research and Standards 4 (No. 1):20 (Jan. 1964)

4. Irwin, G.R., "Analytical Aspects of Crack Stress Field Problems," Univ. of Illinois, TAM Report 213, 1962

5. Griffith, J.R., "Filament-Winding Plastics, Part 4: Syntheses, Properties, and Uses of m-Aminobenzyl Amine (MABA)," NRL Report 6439, Oct. 25, 1966

6. Whisenhunt, F.S., Jr., "Filament-Winding Plastics, Part 2: Role of the Resin in Glass-Fiber-Reinforced Structures Under Tensile Stress," NRL Report 6161, Dec. 1, 1964

7. Greszczuk, L.B., "Elastic Constants and Analysis Methods for Filament Wound Shell Structures," Douglas Aircraft Company, Santa Monica, Report SM-45849, Jan. 1964

8. Wu, E.M., "A Fracture Criterion for Orthotropic Plates Under the Influence of Compression and Shear," Univ. of Illinois, TAM Report 283, 1965